Streptococcus pyogenes Infection and the Human Proteome with a Special Focus on the Immunoglobulin G-cleaving Enzyme IdeS*⑤

Christofer A. Q. Karlsson‡, Sofia Järnum§, Lena Winstedt§, Christian Kjellman§, Lars Björck‡, Adam Linder‡, and Johan A. Malmström‡¶

Infectious diseases are characterized by a complex interplay between host and pathogen, but how these interactions impact the host proteome is unclear. Here we applied a combined mass spectrometry-based proteomics strategy to investigate how the human proteome is transiently modified by the pathogen *Streptococcus pyogenes*, with a particular focus on bacterial cleavage of IgG *in vivo*. In invasive diseases, *S. pyogenes* evokes a massive host response in blood, whereas superficial diseases are characterized by a local leakage of several blood plasma proteins at the site of infection including IgG. *S. pyogenes* produces IdeS, a protease cleaving IgG in the lower hinge region and we find highly effective IdeS-cleavage of IgG in samples from local IgG poor microenvironments. The results show that IdeS contributes to the adaptation of *S. pyogenes* to its normal ecological niches. Additionally, the work identifies novel clinical opportunities for *in vivo* pathogen detection.   *Molecular & Cellular Proteomics 17: 10.1074/mcp.RA117.000525, 1097–1111, 2018.*

The molecular interplay between host and pathogen is complex and under considerable evolutionary pressure. Determining the structure, function and dynamics of all host-pathogen interactions in a systems-wide and quantitative manner is a formidable and fundamental challenge in medical microbiology. A complicating factor is that many bacterial pathogens can cause diverse clinical manifestations, ranging from superficial to invasive disease, expanding the types of interactions. Commonly, local manifestations are confined to highly specific microenvironments like for example mucous layers and epithelial surfaces. In contrast, the development of invasive diseases can result in system-wide spread via the blood stream exposing the disease-causing pathogen to microenvironments associated with high concentrations of antibodies, complement proteins and professional phagocytes. Recent large-scale inventories of the human proteome have revealed that the molecular compositions of common infection sites are highly distinct under healthy conditions (1–3). However, during an infection the molecular composition of these infection sites can be distorted by for example vascular leakage, activation of innate and adaptive immunity and through the infiltration of inflammatory cells. For example, previous large-scale quantitative analysis of the blood plasma proteome in an animal model of sepsis revealed that the blood plasma proteome is profoundly reorganized depending on disease severity (4). In most cases, however, it is unknown whether molecular mechanisms altering the host proteome during an infection are a result of an active host defense or if some of the proteome changes are caused specifically by the infecting pathogen.

In this work, we hypothesized that the transient modulation of the human proteome by bacterial pathogens depends on the state of the host proteome at the infection site and the nature of the virulence factor repertoire of the infecting pathogen. To test this hypothesis, we selected the important bacterial human pathogen *S. pyogenes* as our model system because several molecular mechanisms of virulence are well characterized with an extensive list of confirmed and suggested virulence factors (5–8). *S. pyogenes* infections cause diverse clinical manifestations ranging from mild and common local infections such as tonsillitis, impetigo and erysipelas to life-threating systemic disease like sepsis, meningitis or necrotizing fasciitis. Notably, the incidence of these diseases differs greatly, with more than 600 million cases of tonsillitis and less than 200,000 cases of lethal invasive disease annually (9). As mentioned, these large differences indicate that microenvironments associated with high disease incidence may represent natural habitats where the virulence factor repertoires have evolved to execute their primary functions (10). Consequently, diminishing effective protection by *S. pyogenes* virulence factors in other microenvironments is a possible explanation why cases of severe invasive infections

From the ‡Lund University, Division of Infection Medicine, Department of Clinical Sciences, Solvegatan 19, BMC, Lund, 221 84 Lund, Sweden; §Hansa Medical AB, Scheelevägen 22, 223 63 Lund, Sweden

are rare compared with common superficial and uncomplicated infections.

S. pyogenes has several independent virulence mechanisms that modulate humoral immunity. For example, the cell wall anchored surface proteins M (11) and H have domains that support protein-protein interactions with human host proteins to inhibit phagocytosis, promote adhesion and to secure nutrients from the host (12, 13). In addition, these proteins mediate nonimmune Fc-mediated binding of IgG antibodies resulting in evasion of phagocytosis (14, 15), mostly relevant in IgG-poor environments (16). Furthermore, *S. pyogenes* secretes enzymes associated with different mechanisms to prevent the normal function of IgG. EndoS hydrolyzes the conserved *N*-linked glycan on the heavy chains of human IgG (17), resulting in a reduced affinity to most IgG-Fc receptors (18). SpeB is an unspecific protease capable of cleaving several proteins among them IgG (19). In addition, *S. pyogenes* secretes IdeS, a cysteine protease that specifically cleaves all four subclasses of human IgG in the lower hinge region of the heavy chain, generating one $F(ab')_2$ fragment retaining full antigen-binding activity and one noncovalently linked dimeric Fc fragment (20). As a consequence, IgG antibodies that are bound to the bacterial surface and cleaved by IdeS will lack IgG-Fc receptor and complement binding/activation capability. Apart from implications as an important anti-phagocytic virulence factor (21), IdeS is being developed as a biopharmaceutical drug to temporarily remove pathogenic IgG in autoimmune conditions (22), and is also currently undergoing clinical trials in kidney transplant patients to evaluate its capacity to remove pathogenic donor-specific antibodies and make highly sensitized patients eligible for transplantation (23, 24).

So far, the mode of action for many *S. pyogenes* virulence factors has been determined *in vitro* or in animal studies, whereas few mechanisms have been confirmed to take place in the human host. It can be anticipated that the combined *in vivo* activity of the *S. pyogenes* virulence factor repertoire will introduce differential abundance changes in the human proteome in addition to protein cleavage of both bacterial and human proteins. In this work we have developed novel targeted quantitative mass spectrometry methods to determine the impact of *S. pyogenes* infections on the human proteome with a focus on IgG cleavage at different infection sites. We show that invasive disease caused by *S. pyogenes* results in a systemic molecular host response in the blood plasma, which resembles host responses against other bacterial pathogens. In contrast, *S. pyogenes* causes a highly specific modification of the human proteome through IdeS-mediated proteolytic processing of IgG, which is most pronounced in noninvasive diseases. The results demonstrate that the combined *in vivo* effect of IgG cleavage by IdeS is dependent on the microenvironments associated with different disease and infection types. We anticipate that the proteomics strategy developed and described here can be extended to diseases caused by other bacterial pathogens to investigate the effect of individual virulence factors on host proteomes in patient samples.

EXPERIMENTAL PROCEDURES

Synthetic Peptides and Purified Proteins—Nonpurified synthetic peptides were purchased from JPT Peptide Technologies (Berlin, Germany) or ProteoGenix (Schiltigheim, France). Heavily labeled peptides were purchased from ThermoFisher Scientific (AQUA-grade QuantPro, Waltham, MA).[1] For further details on synthetic and labeled peptides see supplemental Table S2. Recombinant and quantified IdeS was from Hansa Medical AB (23). Human monoclonal IgG subclasses were purchased from Sigma-Aldrich (Darmstadt, Germany).

Human Samples—Serum samples (blood collected with modified CAT serum vacutainer tubes (BD Diagnostics, Franklin Lakes, NJ) containing 2 mM iodoacetic acid) from healthy individuals treated with IdeS were from the Phase I trial NCT01802697 (23). Briefly, subjects were intravenously injected with IdeS (at the following doses: 0.01, 0.04, 0.12, or 0.24 mg IdeS/kg bodyweight), followed by a time-course collection of serum samples. Plasma samples from septic patients were from (48) (blood collected with vacutainer sodium citrate tubes). Plasma samples from healthy individuals were from (49) (blood collected with vacutainer sodium citrate tubes) or were purchased from Innovative Research (pooled normal human plasma, Novi, MI). Swabs and scrapes from local infections from patients with diagnosed *S. pyogenes* infection were collected at Skåne University Hospital or at Laurentiikliniken (a primary health clinic), both in Lund, Sweden. Tonsillar swabs from healthy individuals were obtained at Lund University, Lund Sweden. The medical ethics committee of Lund University approved this study (protocol numbers 2005/790 and 2015/14) and informed consent was obtained from all subjects. The samples were transported at −20 °C and stored at −80 °C until further processing. A compilation of patients, control and IdeS clinical phase I study samples is in supplemental Table S1.

IdeS Endopeptidase Assays—66 pmol of respective purified monoclonal IgG subclass was mixed with 1 pmol IdeS and incubated at 37 °C. Aliquots were removed at time-points 1, 10, and 120 min and enzymatic activity was stopped by denaturing with 8 M urea. For time-points 0 min, IdeS and IgG were mixed in 8 M urea directly. The samples were analyzed with nonreducing SDS-PAGE Criterion TGX Gels (Bio-Rad, Hercules, CA) or SRM (after tryptic digestion, see below). Intact and IdeS-cleaved IgG was calculated by summarizing gel-band intensities. IdeS activity on SDS-PAGE was quantified densitometrically using software GelAnalyzer 2010a. Correlations between SRM and SDS-PAGE were done with linear model methods using the software GraphPad Prism 6.

Sample Preparation—Swab and scrape samples were homogenized using a Fastprep-96 beadbeater (MPBio, Santa Ana, CA) with Lysing Matrix B tubes (MPBio). All protein samples were denatured with 8 M Urea in 100 mM ammonium bicarbonate (ABC) and then reduced with Tris (2-carboxyethyl) phosphine (TCEP) (Sigma-Aldrich) for 1 h at 37 °C, and alkylated with 25 mM iodoacetamide for 45 min

---

[1] The abbreviations used are: AQUA, Absolute quantification; BW, Bodyweight; CRP, C-reactive protein; DDA, Data dependent acquisition; DIA, Data-independent acquisition; EndoS, Endoglycosidase in *Streptococcus pyogenes;* $F(ab')_2$, IgG antigen-binding fragment; Fc, IgG fragment crystallizable region; FDR, False discovery rate; GO, Gene ontology; IdeS, Immunoglobulin G-degrading enzyme of *Streptococcus pyogenes;* IgG, Immunoglobulin G; mAb, Monoclonal antibody; PSM, Peptide spectrum matches; scIgG, Single cleaved IgG; SD, Standard deviation; SpeB, Streptococcal cysteine proteinase; SRM, Selected reaction monitoring; TPP, Trans-proteomic pipeline.

before diluting the sample with 100 mM ABC to a final urea concentration below 1.5 M. Proteins were digested by incubation with trypsin (1/100, w/w) for 10 h at 37 °C. The peptides were desalted and cleaned-up with reversed-phase spin columns (Vydac UltraMicroSpin Silica C18 300Å Columns, Harvard Apparatus, Holliston, MA) according to the manufacturer's instructions.

Data Dependent Acquisition (DDA) and Data Independent Acquisition (DIA)—These peptide analyses were performed on a Q Exactive Plus mass spectrometer (Thermo Scientific) connected to an EASY-nLC 1000 ultra-high-performance liquid chromatography system (Thermo Scientific). Peptides were separated on an EASY-Spray ES802 columns (Thermo Scientific) using a linear gradient from 3 to 35% acetonitrile in aqueous 0.1% formic acid during 2 h. DDA and DIA instrument settings were identical to as described by (4). From the DDA data spectral libraries was built using the workflow described by (50). Briefly, DDA data was searched with the Trans-proteomic pipeline (TPP v4.7 POLAR VORTEX rev 0) with X!Tandem (Jackhammer, 2013.06.15) against Human UniProtKB/Swiss-Prot release 2015_10 canonical sequences (20190 entries) or synthetic peptide sequences (supplemental Table S2) both appended with iRT peptide sequences (51) and reverse decoys. X!Tandem allowed 2 missed peptide cleavages and considered the following modification settings: fixed carbamidomethylation of cysteines, variable oxidation of methionines, variable acetylation of N termini as well as S-carbamoylmethyl-cysteine, cyclization of N-terminal cysteines and pyro-glutamic acid formation from glutamic acid and glutamine. The precursor mass tolerance was set to 20 ppm, and the fragment mass error tolerance was set to 50 ppm. TPP PeptideProphet was used for scoring the X!Tandem search results. The false discovery rate (FDR) was estimated with Mayu (v1.7) and peptide spectrum matches (PSM) were filtered with protein FDR set to 1% resulting in a peptide FDR >1%. Nonredundant consensus spectral libraries were built with TPP Spectrast using the filtered PSMs with all retention times converted to iRTs (51) and selecting the top6 most intensive transitions per assay (tier level 3 analysis).

The human generated spectral library together with a corresponding human decoy spectral library and an iRT spectral library (all deposited at PeptideAtlas) were all used to extract the DIA data from patient samples with the DIANA algorithm v2.0.0 (52). FDR was estimated using PyProphet (DIANA edition 20140527) using the target and decoy spectral library results and the FDR cut-off set to 1% peptide identification and quantification. Proteins or protein groups with single peptide identifications were excluded from further analysis. For protein quantification, the top3 integrated peptide ion intensities extracted from the MS2 spectra was summed up by protein or protein group (53).

Selected Reaction Monitoring (SRM)—The SRM measurements were performed on either TSQ Vantage or TSQ Quantiva triple quadrupole mass spectrometers (Thermo Scientific), connected to EASY-nLC II high-performance liquid chromatography systems (Thermo Scientific). Peptides were separated on columns PicoChip PCH7515–105H354-FS25 (New Objective, Bedford, MA) or EasySpray ES800 (Thermo Scientific), using a linear gradient from 5 to 35% acetonitrile in aqueous 0.1% formic acid during 34 min. In general, instrument dwell time settings were fixed at 10 ms or 40 ms for high respectively low signal intensity peptides, and at scheduled acquisition times defined by iRT normalization (51). SRM assays were obtained from the following publications (16, 25–27), or developed as described by (54). For SRM assay refinement, we tested the assays in plasma or serum backgrounds and selected the best transitions without no signal interference from co-eluting peaks or background noise. Transition lists and tier levels for developed SRM assays are in supplemental Table S2. Transition lists are also available from PanoramaWeb (see supplemental Information). The raw data was processed and analyzed with SRM analysis software Skyline (55), with manual validation and inspection of the results. This included signal intensity, relative fragment ion intensities ratios based on DDA spectral libraries and retention times.

Experimental Design and Statistical Rationale—This study includes 67 serum samples from a phase I clinical trial of IdeS and 61 samples from patients with bacterial infections together with healthy controls. All human sample grouping, time points and type of MS analysis (single replicate analysis with DDA, DIA and/or SRM) are available in supplemental Table S1. DDA and DIA data was searched with target-decoy search strategies to control the FDR (see above). SRM assays targeting Streptococcal IdeS and hinge region peptides from human IgG1–4 (tryptic and semi-tryptic) were developed from recombinant IdeS or pooled synthetic peptides respectfully (supplemental Table S2). SRM assays refined using purified protein samples analyzed in triplicate or duplicate biological replicates. Samples were spiked with heavy isotope-labeled peptides (supplemental Table S2) prior to SRM analysis.

We used hierarchical clustering to analyze associations between patient samples and protein abundances by default distance and spearman linkage method after testing for normality with Shapiro-Wilk's method (null hypothesis rejected, $p < 0.001$). The two major protein clusters (see Fig, 3B) were analyzed with the PANTHER database (56) release 20160715 Overrepresentation Test with GO cellular component complete database using Bonferroni correction for multiple testing. For group-wise comparisons regulated proteins were defined as having a group mean ± fold-change of >5 times and an adjusted p value > 0.05 (Benjamini-Hochberg correction for multiple testing). Statistical analysis of IdeS activity included Pearson correlation coefficient and Wilcoxon's nonparametric test.

RESULTS

Development of an SRM-MS Assay to Measure the Proteolytic Activity of IdeS—Measuring the proteolytic effect by *S. pyogenes* on the entire IgG pool in complex clinical samples, requires new experimental assays to accurately monitor the relationship between intact and fragmented IgG at the subclass level. In this context, it is important to quantify several factors that may influence the degree of IgG cleavage, *i.e.* absolute amounts (mg/ml) of the IgG subclasses, IdeS, plasma proteins of relevance, and quantitative information of other proteases capable of cleaving IgG such as SpeB (Fig. 1A). Because the assessment of IdeS activity entails analysis of samples where the absence is equally important as the presence of a signal, selected reaction monitoring mass spectrometry (SRM-MS) represents a suitable technique. For the construction of an absolute quantification method for IdeS using SRM-MS, we selected crude IdeS SRM-MS peptide-assays (25) and tested the performance of the crude assays in a dilution series of recombinant IdeS spiked in human serum (supplemental Fig. S1). Based on these results, we selected two refined SRM-MS peptide assays (Fig. 1B). For these two peptides we synthesized heavy labeled reference peptides to allow absolute protein quantification. As outlined in Fig. 1A, we also included highly refined SRM-MS peptide assays for selected plasma proteins (26) and a previously developed SRM-MS method to assess the number of *S. pyogenes* cells (27). In this way it becomes possible to correlate the number
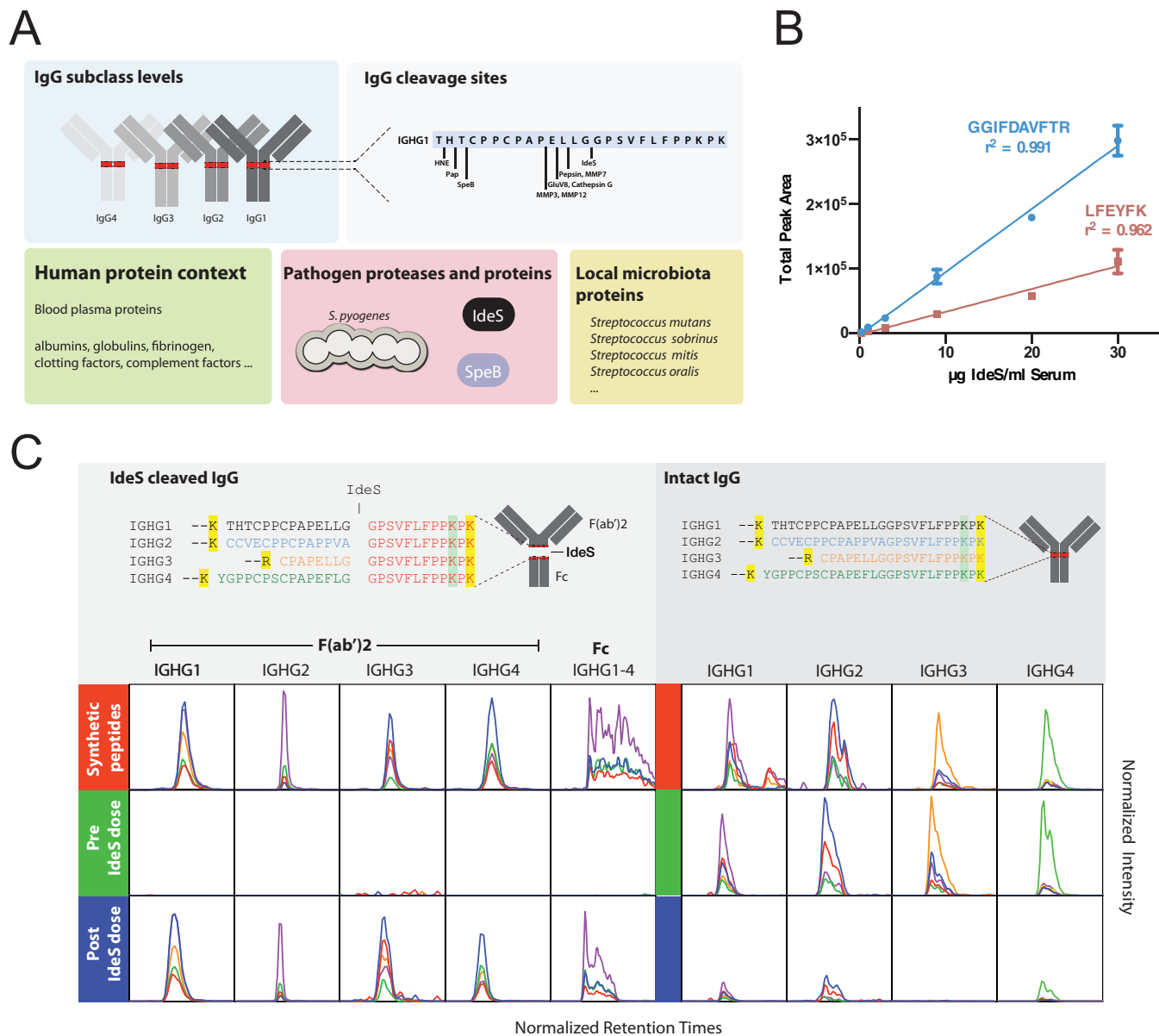
FIG. 1. **Development of SRM assays targeting the proteolytic activity of IdeS on IgG.** *A,* Overview of targeted protein types used for the development of a quantitative SRM assays method to quantify the degree of proteolytic processing of IgG. The SRM method includes all potential IgG peptides produced by the targeted proteases in combination with trypsin. Measuring species-specific pathogen peptides requires knowledge of peptide selectivity and sensitivity across relevant taxa. *B,* Six samples of IdeS at different concentrations in two different human serum backgrounds were prepared by serial dilution to generate a calibration curve spanning a concentration range of 0.25 μg to 30 μg IdeS per ml human serum. The plot shows the total area over the dilution range of indicated SRM targeted peptides derived from IdeS and their respective correlation coefficients (r^2). The data represents average total area $\pm$ S.D. of the two different serum backgrounds. *C,* IdeS cleavage of IgG results in the formation of Fc and F(ab)$_2$ fragments. Tryptic peptides derived from intact IgG or IdeS-cleaved IgG in the lower hinge region spanning the IdeS specific cleavage site in all four subclass heavy chains (UniProt accession entry/residue positions): IGHG1_HUMAN/104–137, IGHG2_HUMAN/101–134, IGHG3_HUMAN/158–185 and IGHG4_HUMAN/101–135) are shown in the upper panels. Yellow or green marked residues indicate a C-terminal trypsin cleavage site or a low probability C-terminal trypsin cleavage site, respectively. The peptide text color indicates the subclass selectivity: black IGHG1, blue IGHG2, orange IGHG3, green IGHG4, redIGHG1–4. Based on synthetic variants of these peptides, SRM assays were developed. In the lower panels are comparisons of the SRM traces from the synthetic peptides (red) and human serum pre- (green) and post- (blue) intravenous administration of IdeS. The *x* axis shows the normalized peptide retention times (iRT score). The *y* axis's ranges are fixed between pre- and post-IdeS doses to show level of change. The line colors represent different product ions depending on the peptide precursor.

of *S. pyogenes* cells to the IgG concentration and the degree of IgG breakdown.

For the construction of SRM-MS peptide assays for all four IgG subclass heavy chains we relied on conserved amino acid sequences as well as the major sequence variations found in the hinge region (Fig. 1*C*). We used both the conserved and variable sequence identities to develop specific SRM-MS peptide assays to quantify total IgG and the individual IgG subclasses (16, 28). These SRM-MS IgG peptide assays with associated heavy labeled reference AQUA peptides targets peptides in the Fc or F(ab′)$_2$ regions of the IgG heavy chain and allows the absolute quantification of the four IgG subclasses as previously shown (16). IdeS is a uniquely specific enzyme cleaving all subclasses of IgG in the lower hinge region (20). To develop SRM-MS peptide assays for determining the ratio between IdeS cleaved and intact IgG, we aligned the lower hinge region sequences spanning the IdeS P1-P1′ cleavage sites (20, 29) of the four subclasses heavy chains, and selected the peptides generated by trypsin cleavage alone and after a combination of both IdeS and trypsin (Fig. 1*C*). Tryptic peptides spanning the IdeS cleavage site were unique for all four subclasses and represent suitable proxies for measuring the amount of intact IgG. Sequential cleavage of IgG using IdeS and trypsin generates unique N-terminal and C-terminal peptide fragments that are identical for all sub-classes (Fig. 1*C*). We targeted all these peptides for the development of SRM-MS assays together with a set of negative control peptides with single negative or positive offset residuals (P2-P1 and P1′-P2′), which are hypothetically not generated by the IdeS and trypsin cleavage combination. As further controls, we also included peptides generated by other known specific proteolytic processing of IgG1 (30) in combination with trypsin digestion as seen in Fig. 1*A*. For more information regarding the development of the SRM-MS assay see supplemental Table S2 and supplemental Figs. S2–S4.

Quantification of the Proportions Between IdeS Cleaved IgG and Intact IgG—Next we used the developed SRM-MS assay to test its selectivity and quantitative performance to measure IgG degradation by IdeS both *in vitro* and *in vivo*. For *in vitro* testing, we used purified human monoclonal IgG antibodies (mAb) of subclass 1–4 and benchmarked the SRM-MS assays by side-by-side comparison with nonreducing SDS-PAGE (supplemental Fig. S2). The results reveal a sequential cleavage of all subclasses with a rapid generation of single cleaved IgG (scIgG) and a slower generation of fully digested IgG (F(ab′)$_2$ fragment) as previously reported (31). IgG3 is cleaved faster compared with the other subclasses and was fully digested after only 10 min of IdeS incubation (supplemental Fig. S2).

To determine the capability of IdeS to cleave IgG in serum provided that sufficient amount of IdeS is available, we used 67 serum samples from a clinical phase I trial (23) (supplemental Table S1). In this trial twenty subjects were infused with 0.01, 0.04, 0.12 or 0.24 mg IdeS per kg bodyweight over 14 or 29 min. The lowest dose corresponds to a theoretical IdeS concentration of ~7 nM (~250 ng/ml, 89.25 aM on column), and is five orders of magnitude lower compared with the levels of human serum albumin (634 μM). This difference in dynamic range is just within the theoretical range of SRM-MS using unfractioned serum or plasma (32). To determine IdeS pharmacokinetics, serum samples of the subjects were collected pre-treatment, directly after administration and at eight time points up to 7 days. First we analyzed the serum concentration of IdeS in these samples starting from the first time points after administration using the optimized SRM-MS peptide assays. Overall the relationship between administered IdeS dose and the serum IdeS concentration was linear although showing an individual variation (Fig. 2*A*). The measured IdeS concentrations depending on dose were in general in agreement with the theoretical values of IdeS serum levels (see Fig. 2*A*) estimated from 3.8% serum per kg bodyweight (BW) (33).

In the same experiment, we quantified the amount of IgG in the time-course samples. Over the time-course experiment there was a clear reduction of the total IgG levels (here defined as the sum of intact IgG and IgG fragments) down to ~40% of the original levels in subjects treated with 0.12 mg/kg BW (Fig. 2*B* and supplemental Table S3). In contrast, and as expected, the levels of IgG in the placebo treated control samples were not affected (Fig. 2*B*). These results indicate that one major effect of intravenous IdeS administration to humans is a reduction of the total IgG levels. This was also confirmed in the phase I trial study using other methods (23). In the same experiments we also measured the level of intact and IdeS cleaved IgG reporter peptides. As shown in Fig. 2*C*, the IdeS truncated subclass F(ab′)$_2$-peptides, representing cleaved IgG, rapidly peaks within the first hour of IdeS administration after which the signal gradually declines. An example of the obtained results with the SRM-MS assays is shown in Fig. 1*C* where targeted peptides show a reverse relationship to the signals from the peptides targeting intact and IdeS cleaved IgG (Fig. 1*A*). Conversely, the intact IgG peptides spanning the cleavage site reduce rapidly in intensity for all the four subclasses with a more pronounced reduction of the IgG3 specific intact peptides. Interestingly, there are only minor differences between the healthy subjects included in the study (Figs. 2*C* and supplemental Fig. S3). By correlating the signal from the subclass specific F(ab′)$_2$-peptides to the intact IgG peptides spanning the cleavage site, it is possible to calculate the degree of cleavage across all the investigated patients (Figs. 2*D* and supplemental Fig. S3). These results show that IdeS consistently increases the ratio between cleaved and intact IgG up to 6 hours after IdeS administration, to a point where >95% of the IgG heavy chains are cleaved, resulting in a completely disrupted IgG pool consisting of Fc, F(ab′)$_2$ and scIgG fragments. The 6-hour time point correlates with a starting decline in the measured levels of IdeS in these
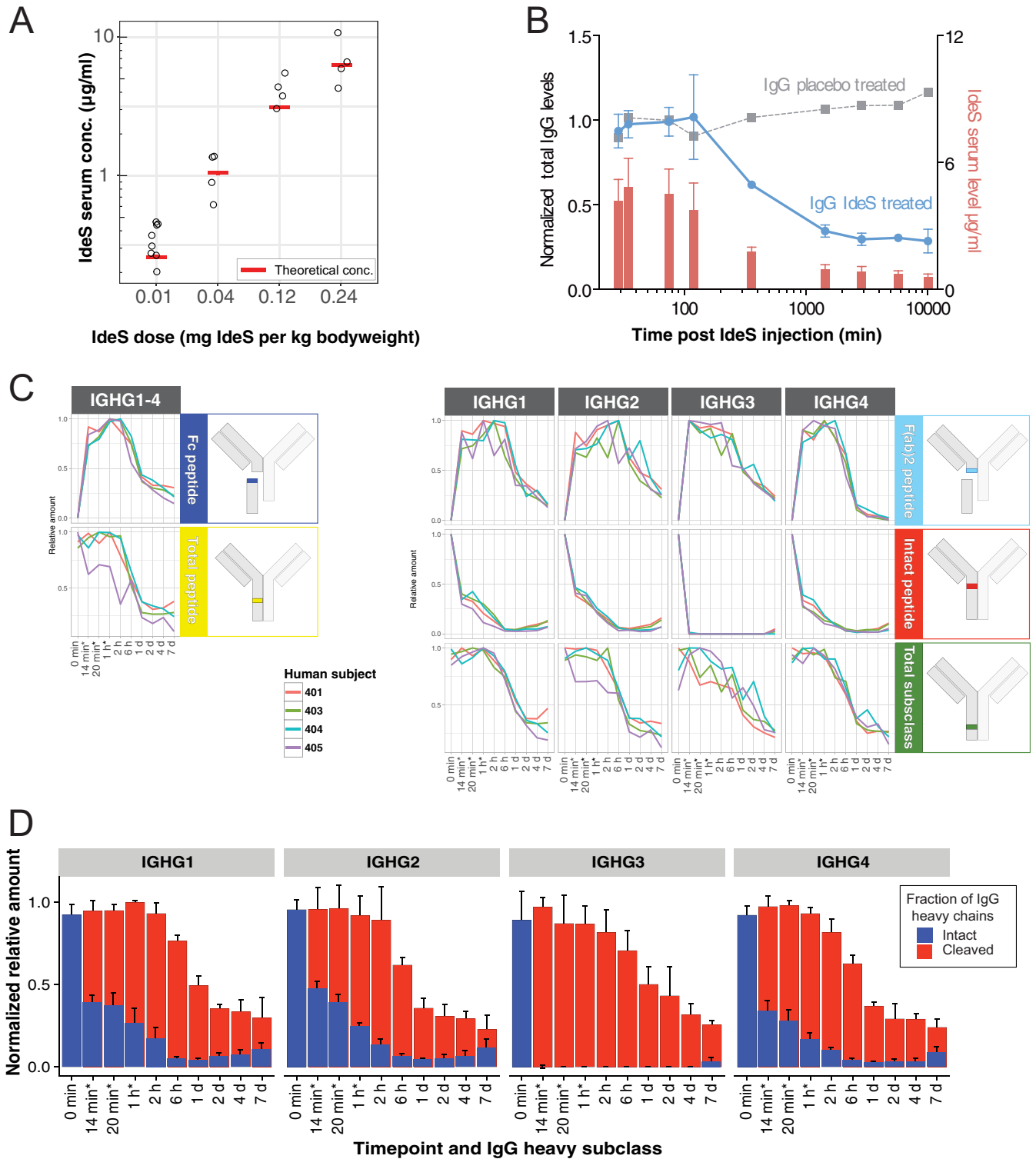
FIG. 2. **Time course of IdeS-cleavage of human IgG *in vivo* measured with SRM.** *A*, The peak serum concentration (left *y* axis) of IdeS across different administered IdeS doses in humans determined with SRM (black circles) and the theoretical serum concentration (red boxes). *B*, The plot shows the average total IgG heavy chain levels (sum of intact and IdeS- cleaved IgG based on peptide DTMSLR intensities normalized to total IgG before IdeS administration, blue, left *y* axis) and IdeS (red, right *y* axis) levels ± S.D. in four individuals treated with 0.12 mg IdeS per kg bodyweight over the time course period. The total IgG of a control individual injected with buffer is shown in gray. *C*, Peptide intensities of total IgG and subclass specific peptide levels of intact and IdeS generated tryptic peptides in four different human subjects over time. Schematic inserts to the right indicate location of the measured peptides. Asterisk marked time points (*) are as follows for subject 401

samples, and with the overall reduction of the concentration of IgG in these samples. Six hours after IdeS administration, there is only a gradual increase of intact IgG over the tested 7 days period. Again, IgG1, 2 and 4 display a similar degree of degradation whereas IgG3 is more sensitive to IdeS cleavage. To estimate the accuracy of the signal from the peptides targeting IdeS activity we searched for peptides potentially generated by offset IdeS cleavage site (non P1-P1′ positions), peptides generated by other proteases than IdeS where the known cleavage sites for IgG1 were obtained from (30), and low probability tryptic peptides variants of the peptides targeting IdeS activity; in this latter case peptides with C termini lacking the PK residues (supplemental Fig. S4). In these experiments we note that these unexpected peptides account for less than 10% of the total signal, and hence that the estimated ratio between cleaved and noncleaved IdeS peptides is within this accuracy range. Collectively, these results demonstrate that IdeS reduces the entire pool of intact IgG up to at least 95% in healthy individuals provided that sufficient amount of IdeS is present.

Proteomics Analysis of Host Response During S. pyogenes Infections—*S. pyogenes* causes a wide range of diseases associated with distinct host microenvironments. However, it currently remains unclear how these microenvironments are altered during an infection and how the specific host-proteomes influence cleavage efficiency of IgG by bacterial proteases. To determine the impact of *S. pyogenes* infections on the human proteome, we swabbed patients with tonsillitis, representing mild and superficial disease, and healthy controls. We also sampled blood plasma from sepsis patients with positive cultures for *S. pyogenes* or other bacterial pathogens, and wound fluid from patients with necrotizing fasciitis, representing invasive and severe disease (Fig. 3*A* and supplemental Table S1). All samples were digested with trypsin and analyzed using data-independent acquisition mass spectrometry analysis (DIA-MS) followed by targeted data analysis (SWATH-MS). The unsupervised hierarchical clustering of the DIA-MS data revealed two distinct sample clusters (Fig. 3*B*). The first sample cluster is comprised of all plasma samples plus three of the wound fluid samples, whereas the second cluster contains all tonsil swabs and the remaining wound fluid samples. As shown in Fig. 3*B*, the two sample clusters have distinctly different proteomes subdivided by two predominant protein clusters. Gene ontology (GO) overrepresentation test identifies an enrichment of intracellular proteins such as cytoskeletal, organelle, nucleus and cytosol proteins in protein cluster 1, and extracellular proteins, including blood plasma and vesicle lumen proteins in protein cluster 2. Pairwise comparison between plasma samples from the healthy controls and all sepsis patients, independent of bacterial pathogen, reveal 98 significantly induced or repressed proteins after correction for multiple hypothesis testing (Figs. 3*C* and 3*E*). The most pronounced change was the increased levels of several acute phase proteins, such as serum amyloid A-1, serum amyloid A-2 and c-reactive protein (CRP) (34), all over 500-fold more abundant in the sepsis patients (supplemental Table S4). On the other extreme, we observe a significant 20–100 fold reduction of several tissue derived proteins such as Myosin-9, ATP synthase subunit beta and 14-3-3 protein gamma, in addition to several known negative acute phase proteins like serum albumin and serotransferrin (34, 35) (31 and 35% reduction respectively). These results show that sepsis drastically distorts the composition of the blood plasma proteome as previously shown in animal models (4). To test if the observed differences were specific for *S. pyogenes,* we performed a pairwise comparison between the sepsis plasma samples positive for *S. pyogenes* and the samples from sepsis patients infected with other bacterial pathogens. This comparison revealed relatively few statistically induced or repressed proteins, although the fold-change for some proteins was substantial (Fig. 3*F*). The large nonsignificant protein fold abundance changes indicate a considerable heterogeneity in host response to sepsis, which is unrelated to pathogen type.

Differential Levels of Plasma Proteins - A Hall Mark of Infection—The incidence of pharyngotonsillitis caused by *S. pyogenes* is a 1000 fold higher compared with invasive *S. pyogenes* infections (9). The reason for this difference in incidence is not clear, but it has been shown that, for example, the IgGFc-binding surface proteins expressed by *S. pyogenes* protect the bacteria against phagocytic killing only in IgG poor microenvironments such as the skin and the oral cavity (16). Comparing the proteomes obtained from tonsil swabs from healthy controls and patients with *S. pyogenes* positive tonsillitis, revealed a significant increase of many proteins in the tonsillitis patients (Fig. 4*A*). On average, the swabbing of tonsil surfaces in patients with tonsillitis has a 6-fold increase in protein mass compared with swabs from healthy controls (see Fig. 4*B* and supplemental Table S4). The pairwise protein abundance t-tests with corrections for multiple testing, shows that the increase in proteome mass observed during tonsillitis is predominately attributed to infiltration of plasma proteins as indicated by the blue colored protein dots in the volcano plot in Fig. 4*A*. Most of the proteins with significantly increased protein levels are extracellular and/or exosomal proteins. In addition, a minor proportion of the increased proteins are associated with cellular structures such actin filament and glycolysis

---

only: 29 min, 35 min, and 75 min respectively. D, Average estimated $\pm$ S.D. levels of intact and IdeS-cleaved IgG at the subclass level after IdeS administration are calculated from measurements in C) (subjects 401, 403–405). Data are normalized to IgG subclass levels before IdeS administration. Asterisk marked time points (*) indicate slightly different time points for subject 401.
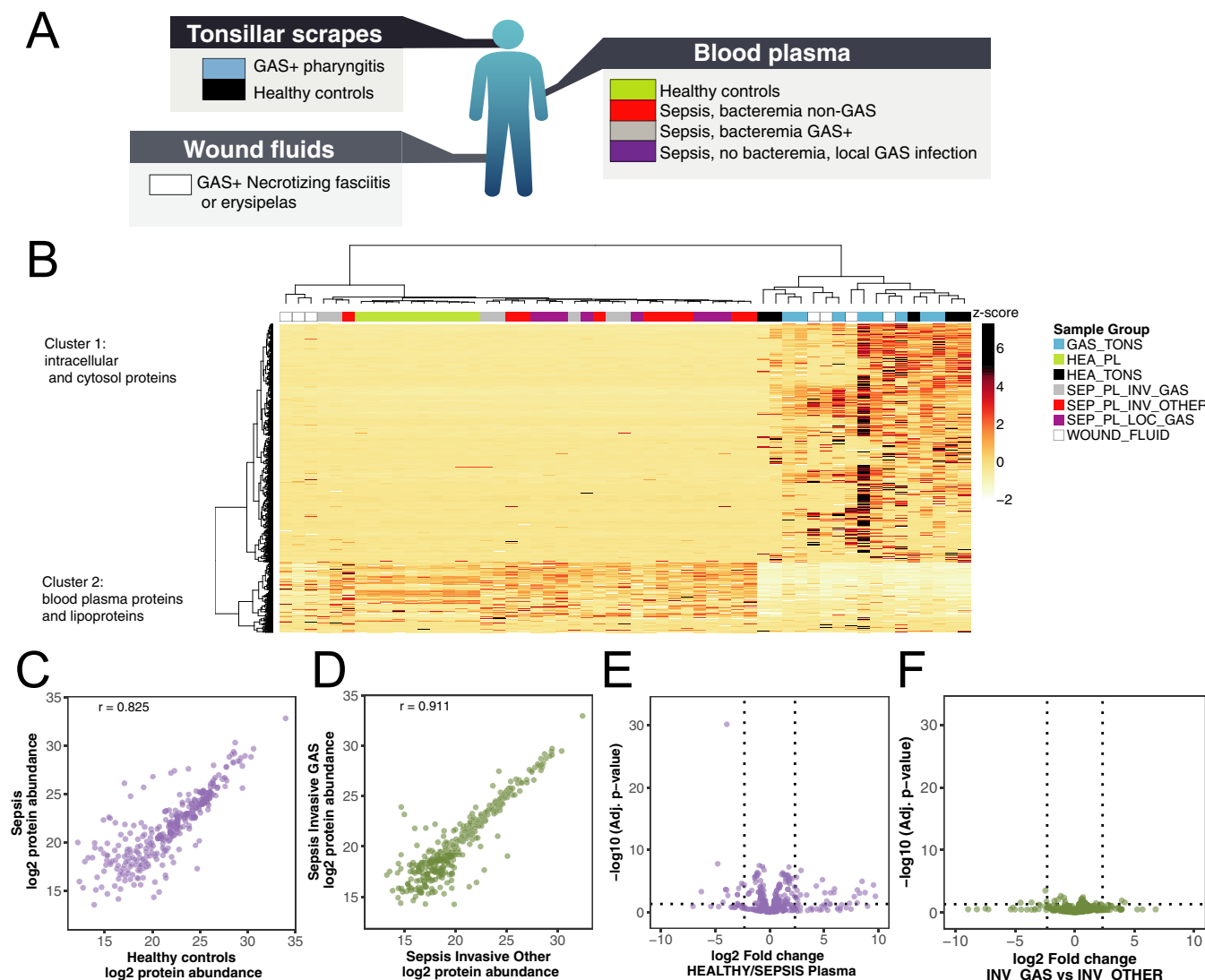
FIG. 3. **Proteomic analysis of human samples.** *A*, Protein samples collected from patients diagnosed with local or systemic *S. pyogenes* infections or from healthy controls, were homogenized and digested with trypsin. Subsequent peptide samples were analyzed with shotgun and Data-independent acquisition (DIA) mass spectrometry-based proteomics workflows. The shotgun data was used for building a reference spectral library for all identified peptides and was used for targeted extraction of the DIA data. *B*, DIA data matrices were normalized by sample total intensities. The heat map shows the relative protein and protein group abundance quantified across samples. Unsupervised clustering using Pearson correlation delineates two major protein clusters and two major patient sample groups. Protein clusters are annotated by statistical overrepresentation test of Gene Ontology cellular component database. The patient samples are colors above based on patient group as same as in *A*. *C–D*, Correlation plots of protein median abundances from selected blood plasma sample groups and with Pearson correlation coefficient (r) indicated. *E–F*, Differential protein abundance volcano plots of selected blood plasma sample groups. Dotted lines indicate significance and fold change thresholds (vertically respectively horizontally). Multiple testing correction was performed by the Benjamini-Hochberg method.

proteins (supplemental Table S4), possibly indicating tissue destruction or increased levels of cell infiltration. Next we analyzed the significantly differentially abundant tonsil proteins ($p < 0.05$) across all sample types. Notably, the overlap between the significantly induced proteins in sepsis and tonsillitis is low (16 of 58/90 proteins respectively), demonstrating that the different disease conditions evoke different host responses. Clustering the significantly altered proteins in tonsillitis samples across all sample types provides a good separation of these samples and

those from healthy controls into two distinct groups (Fig. 4C). However, these proteins have no classification power in sepsis (Fig. 4C, left sample cluster).

Further analysis of the significantly increased plasma proteins during tonsillitis indicates that the plasma leakage is not uniform (Fig. 4D). Based on the extracted ion intensities for the plasma proteins, we estimate an elevation of the plasma concentration at the site of infection from 16% to 28%. When including the increase in protein mass, the actual increase of
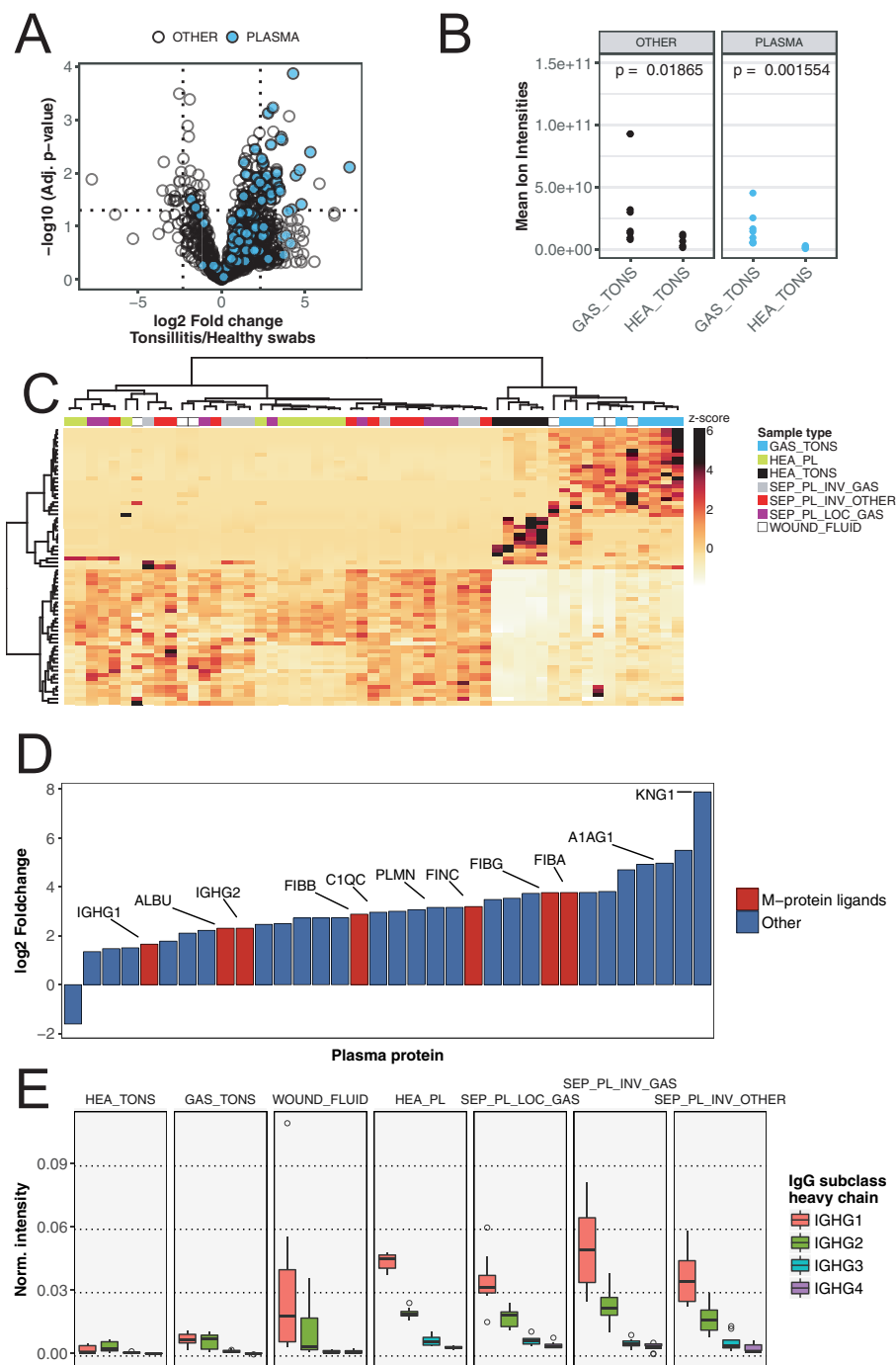
FIG. 4. **Differential abundance of IgG and other blood plasma proteins across patient and control samples.** *A*, Differential protein abundance volcano plots of samples from tonsillar surfaces of *S. pyogenes* pharyngitis patients and healthy controls. Blue filled circles are blood plasma proteins. Dotted lines indicate significance and fold change thresholds (vertically respectively horizontally). Multiple testing corrections were performed by the Benjamini-Hochberg method. *B*, Comparison of mean total protein abundance (sum of all protein ion intensities) of tonsil swabs from patients with *S. pyogenes* pharyngitis (GAS_TONS) and healthy controls (HEA_TONS) showing plasma proteins (same as in *A*)) and other proteins. The *p* values were calculated with nonpaired Wilcoxon rank sum test. *C*, Hierarchical clustering of all patient samples with the subset of proteins that show significantly different abundance on healthy or *S. pyogenes* pharyngitis surfaces (Top left and right quadrants in Fig. 4*A*). *D*, Relative fold-change of plasma proteins with the significantly largest abundance difference between healthy and *S. pyogenes* pharyngitis surfaces (Top left and right quadrants in Fig. 4*A*). Plasma proteins with known binding to *S. pyogenes* M protein are filled with red, and others with blue. Lines and Uniprot Entry name highlight selected proteins with the common suffix "_HUMAN" removed. *E*, Normalized intensities (fraction of total signal) of IgG heavy chain subclasses across sample groups. Boxes represent 25th to 75th % quantiles, middle represents median, and lines smallest and largest observations.

plasma proteins during tonsillitis is in fact 10-fold (Figs. 4*A* and 4*B*). Surprisingly, not all plasma proteins differed significantly between the groups (see Fig. 4*A*), suggesting different propensity of individual plasma proteins to leak into the site of infection. The reason for this differential plasma leakage is not clear, but it is independent of plasma protein mass as there is no correlation between fold change and protein mass (data not shown). It is well established that *S. pyogenes* can bind numerous plasma proteins to its surface. The important *S. pyogenes* virulence factor M1 protein can for example bind fibrinogen (36, 37), albumin (15, 38) and fibronectin (39) to inhibit phagocytosis (40) and facilitate uptake of fatty acids (13). In our study, all known M1 protein interacting plasma proteins are among the top 30 proteins with the highest fold change during tonsillitis, as indicated by red bars in Fig. 4*D*. The increased levels of these proteins at the site of infection may enable *S. pyogenes* to exploit these proteins to promote immune evasion. Alternatively, these proteins may be retained better at the site of infection possibly via their interaction with the streptococcal surface.

Because the efficiency of IgGFc-binding to M1 protein is dependent on IgG concentration, we investigated the IgG concentration in the different sample types. In the plasma samples the concentration of IgG is high, and sepsis does not introduce any major changes in IgG concentration or subclass distribution. The concentration of IgG is also on average high in wound fluid samples, although there is a considerable degree of variability in these samples. In contrast the tonsil swabs contain much lower amounts of IgG with higher levels of IgG during tonsillitis compared with the healthy controls (Fig. 4*D*–4*E*). Throughout all the analyzed samples we note that the subclass distribution is not altered by *S. pyogenes.*

IdeS Activity in Patients with S. pyogenes Infection—In the following experiments we analyzed the samples outlined in Fig. 3*A* (supplemental Table S1) using LC-SRM MS to quantify the absolute level of IgG cleavage in these samples (see supplemental Figs. S5, S7 and supplemental Table S5). Absolute quantification of IgG confirms that the IgG concentration is drastically different between site samples with high concentration of IgG in plasma samples and in some of the wound fluid samples (Figs. 5*A* and 5*B)*. These samples exhibit a concentration of around 1 pmol/μl of IgG1, with an expected subclass distribution. The tonsil swabs have around 10 to 100-fold lower concentration of IgG compared with the plasma samples. The swabs from the tonsillitis patients have higher concentration of IgG compared with the swabs from the healthy volunteers, mostly pronounced for IgG1, because of increased plasma leakage as shown in Fig. 4 This increase in plasma leakage was supported by the elevated levels of several other high abundant plasma proteins such as albumin and fibrinogen in the swabs from the tonsillitis patients (Figs. 4*B* and 5*A*).

The tonsil swabs from tonsillitis patients have elevated levels of IgG, but still there is a considerable degree of IgG cleavage in these samples. All seven samples reveal signs of IdeS specific IgG cleavage, and in some cases specific subclasses are cleaved to 100%. Although IgG3 tends to be more sensitive to IdeS cleavage, the differences between the subclasses are not significant. Surprisingly, we also observe detectable levels of cleaved IgG in the IgG rich samples such as some of the wound fluids and plasma sample from patients infected with *S. pyogenes*, but not in plasma from patients with sepsis caused by other bacterial pathogens. There are also trace levels of cleaved IgG in plasma from patients with sepsis with a confirmed local *S. pyogenes* infection but void of detectable levels of the bacterium in plasma determined using conventional culturing techniques. Notably peptides hypothetically derived from other defined IgG1 proteases were detected in several samples. However, the peptide intensities generally correlated to the total IgG1 levels ($r = \geq 0.55$, $p > 0.001$). This contrasted with IdeS-derived IgG1peptides which did not correlate with the total IgG1 heavy chain levels ($r = 0.07$, $p = 0.73$) (supplemental Figs. S6*A* and S6*B*). In addition, the only IgG1 heavy chain peptide with large significant mean difference between *S. pyogenes* positive samples groups as compared with negative control groups, was the IdeS-derived peptide (supplemental Fig. S6*C*). Combined these results demonstrate that IdeS cleavage of IgG either occurs locally or directly in the blood plasma and thereby noticeably alter the integrity of the complete IgG repertoire, and that the signals from IdeS cleavage IgG products are unique for samples from individuals infected by *S. pyogenes*.

To further explore the reason for the observed differential cleavage of IgG, we used a previously established *S. pyogenes* specific mass spectrometry-based cell count method (27). With this method we observe detectable levels of *S. pyogenes* directly in three of the seven tonsillitis patients, with a pronounced signal in two patients. Similarly, the swabs from two of the three patients with necrotizing fasciitis revealed measurable levels of *S. pyogenes*. As expected, there were no detectable *S. pyogenes* specific peptides in the tonsil swab from healthy controls (see green panels in Figs. 5*A* and 5*B*). In most of these samples we detect peptides specific for the *Streptococcus* genus reflecting the composition of the oral microbiota. Correlation analysis between the number of *S. pyogenes* cells and the degree of IgG cleavage reveal no correlation (data not shown). Surprisingly, we were unable to detect IdeS or SpeB in any of the samples and consequently it is not possible to correlate the degree of IgG cleavage to the level of IdeS or to determine if some of the *S. pyogenes* strains secrets higher concentration of IdeS. Furthermore, we are unable to rule out that the differences in cleavage may be attributed to neutralizing antibodies or other unknown factors influencing IdeS cleavage efficiency. Based on these results we conclude that lower absolute concentration of IgG and
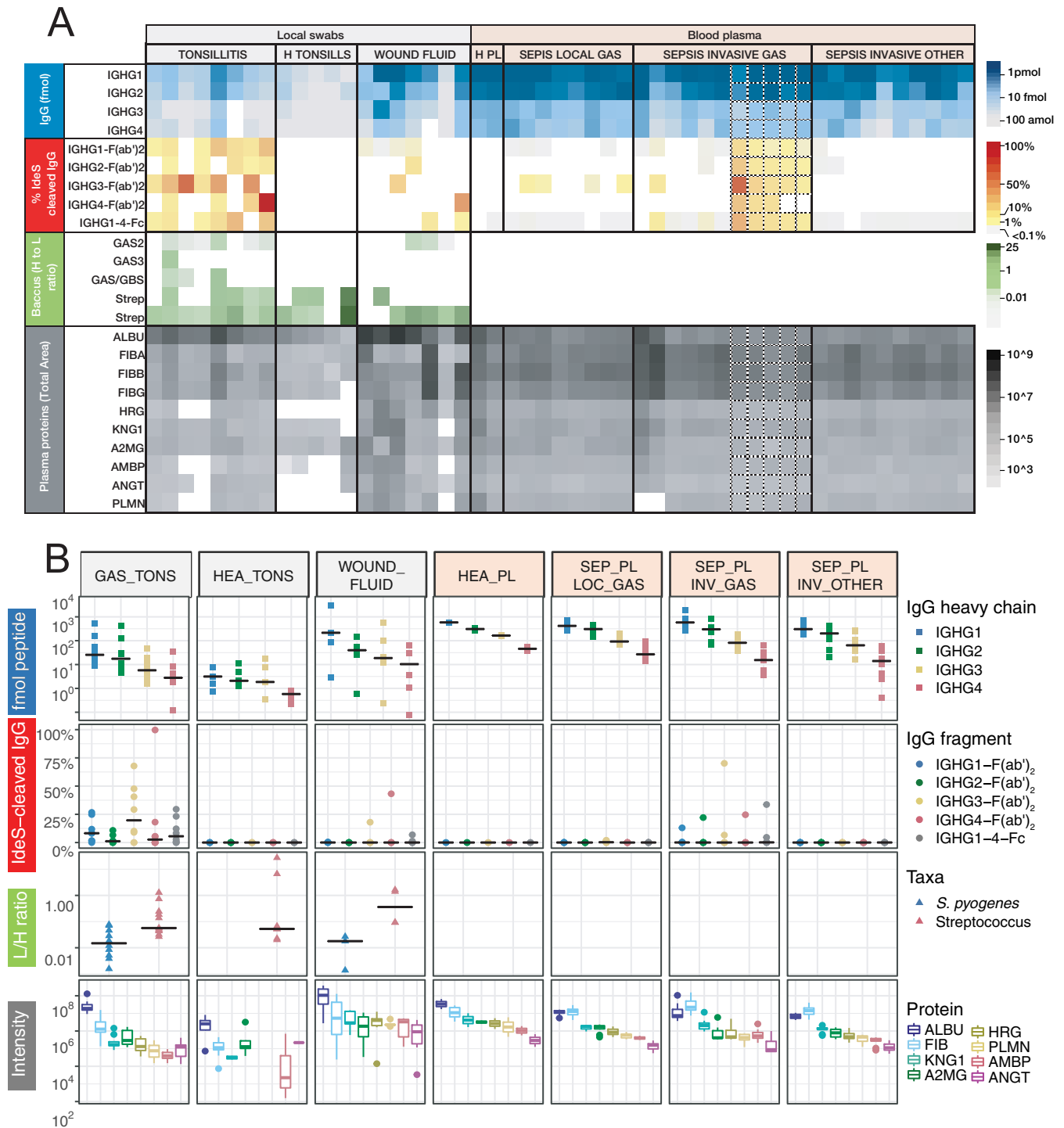
FIG. 5. **Analysis of IdeS-cleaved IgG and other targeted proteins in patient and control samples.** The digested patient samples from Fig. 3*A* were analyzed using the SRM-MS method show in Fig. 1*A*. *A*, Each column represents a human sample collected either from a local infection, plasma from blood samples drawn from patients diagnosed with bacterial sepsis, or healthy control samples. Columns with dotted line borders are time series samples from a single patient (see supplemental Table S1). Blue panel shows the absolute concentration of total IgG. Red panel shows the proportion of IdeS-cleaved IgG. Green panel shows the levels of peptides specific for the *S. pyogenes* species or for the Streptococcus genus. Gray panel show the intensities of peptides derived from human plasma proteins. Abbreviations indicate the Uniprot Entry name with the common suffix "_HUMAN" removed. *B*, Shows the same data as in *A*, but by sample group and only the first time point. Black lines indicate the group median value of *y* axis values.

detectable levels of *S. pyogenes* cells are the predominant factors for proportionally high levels of IgG cleavage.

In conclusion, the novel SRM-MS assay identifies active IdeS-mediated degradation of IgG in all samples from patients with a confirmed *S. pyogenes* infection. At the local site of infection, we can quantify low levels of peptides unique for *S. pyogenes* although IdeS is present in amounts below the detection level. These results demonstrate that the *in vivo* activity of a low abundant and undetectable protease can comprise part of the IgG pool with a higher cleavage efficiency in microenvironments associated with low IgG concentrations.

DISCUSSION

The aim of the present study was to investigate how the human proteome is influenced by *S. pyogenes* infections, locally and during invasive disease. Here, we applied a combined mass spectrometry strategy to a set of swabs from local infections and sepsis blood plasma and wound fluids from patients with invasive disease to address this question. The results show that sepsis results in a dramatic change in the blood plasma proteome composition compared with healthy conditions. Some of the proteins with significant changes are known markers for inflammation (acute phase proteins) and are expected to increase or decrease because of the disease. However, when comparing sepsis caused by *S. pyogenes* with other bacterial pathogens the difference was minor. Sepsis is a serious and life-threatening condition but only constitutes a minor part of all *S. pyogenes* infections. *S. pyogenes* most common habitat is the human pharynx, where it either causes infection or resides asymptomatically. In asymptomatic carriers, the bacteria are exposed to low levels of blood plasma proteins originating from saliva and mucosal secretions, whereas during tonsillitis/pharyngitis, the inflammation will cause exudation of plasma proteins to the epithelial surface. Here we detect a 10-fold increase of many plasma proteins in the swabs from patients with *S. pyogenes* tonsillitis, including plasma proteins known to interact with *S. pyogenes* surface proteins. Because the increase of individual plasma proteins is not dependent on molecular mass, the pattern is not explained simply by plasma leakage, but rather by the binding and retainment of proteins at the surface of infecting *S. pyogenes* bacteria.

Based on the novel SRM-based IgG quantification assay, we could confirm that IdeS hydrolyzes IgG during a human *S. pyogenes* infection, and that the cleavage efficiency is highly variable depending on the site of infection. On average, the highest levels of IdeS-cleaved IgG are found in tonsillitis samples, much higher than in plasma from sepsis patients. This is expected considering the lower concentrations of IgG at the site of a local infection compared with vascular IgG levels. Previous work (21) has shown that IdeS cleavage of IgG antibodies bound to the surface of *S. pyogenes* protects the bacteria against phagocytic killing *in vitro*. The natural eco-logical niche for *S. pyogenes* is the throat with a low concentration of IgG (saliva), and in this environment the amount of IdeS is sufficient to remove opsonizing IgG, whereas in the bloodstream the concentration of IgG is most likely too high compared with the concentration of IdeS. Because *S. pyogenes* is not adapted to blood and invasion of the bloodstream by *S. pyogenes* is very rare, this makes sense from an evolutionary point of view (16). In this work we find that the IgG3 subclass is most susceptible to IdeS cleavage *in vitro*, as well as in the IdeS clinical trial on healthy volunteers and during *S. pyogenes* infection *in vivo*. IgG3 has been proposed to be the first IgG subclass to emerge after IgM isotype switching and involved in the early humoral response against pathogens (41). Moreover, IgG3 has the highest affinity for complement factor C1q (42). Hypothetically, IdeS has evolved primarily to target IgG3 functions, but the results could also be because of IgG3's inherent lower half-life and increased susceptibility to hinge-region proteolysis (43).

When recombinant IdeS is intravenously administered to healthy humans, the total IgG pool is rapidly cleaved (23) (Fig. 2). However, in this case the concentration of IdeS ($\sim$6 μg/ml) is orders of magnitude higher than what can be expected during an infection with *S. pyogenes*. To exemplify; the mass of a streptococcal cell (dry weight) is 0.2 pg of which 55% is protein. With a high bacterial load of 10^3 bacteria per ml blood, this corresponds to 110 pg of *S. pyogenes* total protein per ml blood. Although the enzyme and substrate dynamics are different during an infection with IdeS production over time and perhaps reaching a steady-state concentration of the protease, the concentration will be substantially lower than what is required for the cleavage of the entire IgG pool. IdeS is a uniquely specific protease, apart from IgG no other substrate has been identified, and based on current knowledge, the cleavage sites in IgG heavy chains are also unique for IdeS (30). The present work shows that IdeS activity above background levels ($>$0.1% cleavage) strongly correlates with *S. pyogenes* infection. It is most likely that IdeS is present during *S. pyogenes* infection because the *ideS* gene is present in most serotypes of *S. pyogenes* (44) and serum samples from individuals following *S. pyogenes* infection contain anti-IdeS antibodies (45). Furthermore, screening of 208 serum samples from healthy humans showed that $>$95% have detectable levels of anti-IdeS antibodies (23), showing that most humans have been infected with IdeS-producing *S. pyogenes* stains during their life-time. There are several other bacterial and eukaryotic proteases that hydrolyze IgG in the hinge region, but not at the same residual sites as IdeS (30). However, it cannot be excluded that so far uncharacterized IdeS-like enzymes might be produced by other members of the microbiota at epithelial surfaces colonized by *S. pyogenes*, or that IdeS-like Fc and F(ab)$_2$ fragments could be generated by nonspecific cleavage by broad-spectrum human proteases

released as part of the inflammatory response to *S. pyogenes* infection.

The SRM-method estimates the percentage of IdeS-cleaved IgG based on fragment-ion relative intensities of the light and heavy isotope-labeled versions of quantified peptides spiked into the samples. Heavy labeled peptides (AQUA peptides) represent the gold-standard for peptide quantification, although this quantification has its limitations and drawbacks (46). The heavy peptides do not account for differences in the proteolytic cleavage efficacy or peptide loss in the sample preparation step. Hence the relationship between inherent peptide and the original protein levels may not be equimolar (47). This effect is likely amplified in our study as our method requires two peptide pairs to calculate the amounts of IdeS-cleaved IgG. Normally SRM-based quantification involves selection of optimal peptides to represent their parent protein. When measuring IdeS activity on IgG as performed here, the target peptides were predetermined by the selectivity of IdeS cleavage of the lower hinge region of IgG, which gives no option to discard suboptimal peptides. We tried to circumvent these limitations by making calibrations curves with known levels of intact and cleaved IgG. However, this indirect mode of measuring IdeS activity is likely associated with errors in the quantification. Previous method of measuring IdeS activity is performed by for example densitometric measurements of stained bands on SDS-PAGE gels or ELISA assays. Still, the SRM method developed here is clearly associated with improved quantitative accuracy and dynamic range, and, which is important in relation to this study, the method offers the possibility of measuring several related aspects such as levels of IdeS, absolute amount of IgG and other plasma proteins, and additional cleavage patterns known to compromise the structure of IgG.

In future work we anticipate that the combined MS based strategy proposed here can serve as a blueprint for other studies aiming at identifying the impact of bacterial proteolytic activity on human proteins. In these studies, searching for non- or semi-tryptic peptides that increase in concentration after exposing human proteins to live bacteria can serve as targets for down-stream DIA-MS analysis. As many bacterial proteases are not as specific as IdeS these efforts may require a large set peptide assay that are monitored in for example DIA-MS. In this context it is important to point that comparative analysis of the cleaved IgG peptides between SRM and DIA performed here demonstrate a good correlation as shown in supplemental Fig. S7. Once informative peptides have been identified these could subsequently be targeted by SRM to quantify the *in vivo* effect of bacterial proteases on human proteins. In summary, the work presented here provides a novel experimental approach to investigate the effect of a significant bacterial pathogen on the human proteome in different clinical conditions; asymptomatic colonization, localized superficial infection and invasive disease. In addition, the analysis of the IgG degrading activity of IdeS in healthy individuals and patients infected with *S. pyogenes,* shows that the specific activity of a bacterial protease can be used to diagnose and follow/evaluate the progression of an ongoing infection and also makes IdeS a promising vaccine candidate. This provides new scientific opportunities with considerable clinical and theoretical potential.

DATA AVAILABILITY

The MS raw data, MS search parameters and applied analysis results are deposited at PeptideAtlas: http://www.peptideatlas.org/PASS/PASS01096 and PanoramaWeb: https://panoramaweb.org/labkey/xanZMv.url.

Ⓢ This article contains supplemental material.

¶ To whom correspondence should be addressed: Lund University, Division of Infection Medicine, Department of Clinical Sciences, Solvegatan 19, BMC D13, 221 84 Lund, Sweden. Tel.: +46 46 222 08 30; E-mail: johan.malmstrom@med.lu.se.

REFERENCES

1. Kim, M.-S., Pinto, S. M., Getnet, D., Nirujogi, R. S., Manda, S. S., Chaerkady, R., Madugundu, A. K., Kelkar, D. S., Isserlin, R., Jain, S., Thomas, J. K., Muthusamy, B., Leal-Rojas, P., Kumar, P., Sahasrabuddhe, N. A., Balakrishnan, L., Advani, J., George, B., Renuse, S., Selvan, L. D. N., Patil, A. H., Nanjappa, V., Radhakrishnan, A., Prasad, S., Subbannayya, T., Raju, R., Kumar, M., Sreenivasamurthy, S. K., Marimuthu, A., Sathe, G. J., Chavan, S., Datta, K. K., Subbannayya, Y., Sahu, A., Yelamanchi, S. D., Jayaram, S., Rajagopalan, P., Sharma, J., Murthy, K. R., Syed, N., Goel, R., Khan, A. A., Ahmad, S., Dey, G., Mudgal, K., Chatterjee, A., Huang, T.-C., Zhong, J., Wu, X., Shaw, P. G., Freed, D., Zahari, M. S., Mukherjee, K. K., Shankar, S., Mahadevan, A., Lam, H., Mitchell, C. J., Shankar, S. K., Satishchandra, P., Schroeder, J. T., Sirdeshmukh, R., Maitra, A., Leach, S. D., Drake, C. G., Halushka, M. K., Prasad, T. S. K., Hruban, R. H., Kerr, C. L., Bader, G. D., Iacobuzio-Donahue, C. A., Gowda, H., and Pandey, A. (2014) A draft map of the human proteome. *Nature* **509,** 575–581

2. Wilhelm, M., Schlegl, J., Hahne, H., Moghaddas Gholami, A., Lieberenz, M., Savitski, M. M., Ziegler, E., Butzmann, L., Gessulat, S., Marx, H., Mathieson, T., Lemeer, S., Schnatbaum, K., Reimer, U., Wenschuh, H.,

Mollenhauer, M., Slotta-Huspenina, J., Boese, J.-H., Bantscheff, M., Gerstmair, A., Faerber, F., and Kuster, B. (2014) Mass-spectrometry-based draft of the human proteome. *Nature* **509,** 582–587

3. Uhlén, M., Oksvold, P., Fagerberg, L., Lundberg, E., Jonasson, K., Forsberg, M., Zwahlen, M., Kampf, C., Wester, K., Hober, S., Wernerus, H., Björling, L., and Ponten, F. (2010) Towards a knowledge-based Human Protein Atlas. *Nat. Biotechnol.* **28,** 1248–1250

4. Malmström, E., Kilsgård, O., Hauri, S., Smeds, E., Herwald, H., Malmström, L., and Malmström, J. A. (2016) Large-scale inference of protein tissue origin in gram-positive sepsis plasma using quantitative targeted proteomics. *Nat. Commun.* **7,** 10261

5. Musser, J. M., and Shelburne, S. A. (2009) A decade of molecular pathogenomic analysis of group A Streptococcus. *J. Clin. Invest.* **119,** 2455–2463

6. Bisno, A. L., Brito, M. O., and Collins, C. M. (2003) Molecular basis of group A streptococcal virulence. *Lancet Infectious Dis.* **3,** 191–200

7. Cunningham, M. W. (2000) Pathogenesis of group A streptococcal infections. *Clin. Microbiol. Rev.* **13,** 470–511

8. Cole, J. N., Barnett, T. C., Nizet, V., and Walker, M. J. (2011) Molecular insight into invasive group A streptococcal disease. *Nat. Rev. Microbiol.* **9,** 724–736

9. Carapetis, J. R., Steer, A. C., Mulholland, E. K., and Weber, M. (2005) The global burden of group A streptococcal diseases. *Lancet Infectious Dis.* **5,** 685–694

10. Wollein Waldetoft, K., and Råberg, L. (2014) To harm or not to harm? On the evolution and expression of virulence in group A streptococci. *Trends Microbiol.* **22,** 7–13

11. Fischetti, V. A. (1989) Streptococcal M protein: molecular design and biological behavior. *Clin. Microbiol. Rev.* **2,** 285–314

12. Carlsson, F., Berggård, K., Stålhammar-Carlemalm, M., and Lindahl, G. (2003) Evasion of phagocytosis through cooperation between two ligand-binding regions in Streptococcus pyogenes M protein. *J. Exp. Med.* **198,** 1057–1068

13. Malmström, J. A., Karlsson, C., Nordenfelt, P., Ossola, R., Weisser, H., Quandt, A., Hansson, K., Aebersold, R., Malmström, L., and Björck, L. (2011) Streptococcus pyogenes in human plasma: adaptive mechanisms analyzed by mass spectrometry based proteomics. *J. Biol. Chem.* **287,** 1415–1425

14. Heath, D. G., and Cleary, P. P. (1989) Fc-receptor and M-protein genes of group A streptococci are products of gene duplication. *Proc. Natl. Acad. Sci. U.S.A.* **86,** 4741–4745

15. Åkesson, P., Schmidt, K. H., Cooney, J., and Björck, L. (1994) M1 protein and protein H: IgGFc- and albumin-binding streptococcal surface proteins encoded by adjacent genes. *Biochem. J.* **300,** 877–886

16. Nordenfelt, P., Waldemarson, S., Linder, A., Mörgelin, M., Karlsson, C., Malmström, J. A., and Björck, L. (2012) Antibody orientation at bacterial surfaces is related to invasive infection. *J. Exp. Med.* **209,** 2367–2381

17. Collin, M., and Olsén, A. (2001) EndoS, a novel secreted protein from Streptococcus pyogenes with endoglycosidase activity on human IgG. *EMBO J.* **20,** 3046–3055

18. Allhorn, M., Olin, A. I., Nimmerjahn, F., and Collin, M. (2008) Human IgG/FcγR interactions are modulated by Streptococcal IgG glycan hydrolysis. *PLoS ONE* **3,** e1413

19. Collin, M., Svensson, M. D., Sjöholm, A. G., Jensenius, J. C., Sjöbring, U., and Olsen, A. (2002) EndoS and SpeB from Streptococcus pyogenes inhibit immunoglobulin-mediated opsonophagocytosis. *Infect. Immun.* **70,** 6646–6651

20. Pawel-Rammingen von, U, Johansson, B. P., and Björck, L. (2002) IdeS, a novel streptococcal cysteine proteinase with unique specificity for immunoglobulin G. *EMBO J.* **21,** 1607–1615

21. Pawel-Rammingen von, U, Johansson, B. P., Tapper, H., and Björck, L. (2002) Streptococcus pyogenes and phagocytic killing. *Nat. Med.* **8,** 1044–1045

22. Collin, M., and Björck, L. (2017) Toward Clinical use of the IgG Specific Enzymes IdeS and EndoS against Antibody-Mediated Diseases. *Methods Mol. Biol.* **1535,** 339–351

23. Winstedt, L., Järnum, S., Nordahl, E. A., Olsson, A., Runström, A., Bockermann, R., Karlsson, C., Malmström, J. A., Palmgren, G. S., Malmqvist, U., Björck, L., and Kjellman, C. (2015) Complete removal of extracellular IgG antibodies in a randomized dose-escalation phase I study with the bacterial enzyme IdeS - A novel therapeutic opportunity. *PLoS ONE* **10,** e0132011

24. Jordan, S. C., Lorant, T., Choi, J., Kjellman, C., Winstedt, L., Bengtsson, M., Zhang, X., Eich, T., Toyoda, M., Eriksson, B.-M., Ge, S., Peng, A., Järnum, S., Wood, K. J., Lundgren, T., Wennberg, L., Bäckman, L., Larsson, E., Villicana, R., Kahwaji, J., Louie, S., Kang, A., Haas, M., Nast, C., Vo, A., and Tufveson, G. (2017) IgG Endopeptidase in highly sensitized patients undergoing transplantation. *N. Engl. J. Med.* **377,** 442–453

25. Karlsson, C., Malmström, L., Aebersold, R., and Malmström, J. A. (2012) Proteome-wide selected reaction monitoring assays for the human pathogen Streptococcus pyogenes. *Nat. Commun.* **3,** 1301

26. Sjöholm, K., Karlsson, C., Linder, A., and Malmström, J. A. (2014) A comprehensive analysis of the Streptococcus pyogenes and human plasma protein interaction network. *Mol. Biosyst.* **10,** 1698–1708

27. Sjöholm, K., Kilsgård, O., Teleman, J., Happonen, L., Malmström, L., and Malmström, J. A. (2017) Targeted proteomics and absolute protein quantification for the construction of a stoichiometric host-pathogen surface density model. *Mol. Cell. Proteomics* **16,** S29–S41

28. Hong, Q., Lebrilla, C. B., Miyamoto, S., and Ruhaak, L. R. (2013) Absolute quantitation of immunoglobulin G and its glycoforms using multiple reaction monitoring. *Anal. Chem.* **85,** 8585–8593

29. Wenig, K., Chatwell, L., Pawel-Rammingen, von, U., Björck, L., Huber, R., and Sondermann, P. (2004) Structure of the streptococcal endopeptidase IdeS, a cysteine proteinase with strict specificity for IgG. *Proc. Natl. Acad. Sci. U.S.A.* **101,** 17371–17376

30. Brezski, R. J., and Jordan, R. E. (2010) Cleavage of IgGs by proteases associated with invasive diseases: an evasion tactic against host immunity? *MAbs* **2,** 212–220

31. Vindebro, R., Spoerry, C., and Pawel-Rammingen von, U. (2013) Rapid IgG heavy chain cleavage by the streptococcal IgG endopeptidase IdeS is mediated by IdeS monomers and is not due to enzyme dimerization. *FEBS Lett.* **587,** 1818–1822

32. Mitchell, P. (2010) Proteomics retrenches. *Nat. Biotechnol.* **28,** 665–670

33. Morgan, G. (2005) *Clinical Anesthesiology* (McGraw-Hill Professional)

34. Davidson, S. J. (2013) Inflammation and acute phase proteins in haemostasis. *InTech*

35. Ritchie, R. F., Palomaki, G. E., Neveux, L. M., Navolotskaia, O., Ledue, T. B., and Craig, W. Y. (1999) Reference distributions for the negative acute-phase serum proteins, albumin, transferrin and transthyretin: a practical, simple and clinically relevant approach in a large cohort. *J. Clin. Lab. Anal.* **13,** 273–279

36. Kantor, F. S. (1965) Fibrinogen precipitation by Streptococcal M protein. I. Identity of the reactants, and stoichiometry of the reaction. *J. Exp. Med.* **121,** 849–859

37. Sanford, B. A., Davison, V. E., and Ramsay, M. A. (1982) Fibrinogen-mediated adherence of group A Streptococcus to influenza A virus-infected cell cultures. *Infect. Immun.* **38,** 513–520

38. Myhre, E. B., and Kronvall, G. (1980) Demonstration of specific binding sites for human serum albumin in group C and G streptococci. *Infect. Immun.* **27,** 6–14

39. Schmidt, K. H., Mann, K., Cooney, J., and Köhler, W. (1993) Multiple binding of type 3 streptococcal M protein to human fibrinogen, albumin and fibronectin. *FEMS Immunol. Med. Microbiol.* **7,** 135–143

40. Carlsson, F., Sandin, C., and Lindahl, G. (2005) Human fibrinogen bound to Streptococcus pyogenes M protein inhibits complement deposition via the classical pathway. *Mol. Microbiol.* **56,** 28–39

41. Collins, A. M., and Jackson, K. J. L. (2013) A temporal model of human IgE and IgG antibody function. *Front. Immunol.* **4,** 235

42. Schroeder, H. W., and Cavacini, L. (2010) Structure and function of immunoglobulins. *J. Allergy Clin. Immunol.* **125,** S41–S52

43. Carter, P. J. (2006) Potent antibody therapeutics by design. *Nat. Rev. Immunol.* **6,** 343–357

44. Pawel-Rammingen von, U. (2012) Streptococcal IdeS and its impact on immune response and inflammation. *J. Innate Immun.* **4,** 132–140

45. Åkesson, P., Moritz, L., Truedsson, M., Christensson, B., and Pawel-Rammingen, von, U. (2006) IdeS, a highly specific immunoglobulin G (IgG)-cleaving enzyme from Streptococcus pyogenes, is inhibited by specific IgG antibodies generated during infection. *Infect. Immun.* 74, 497–503

46. Picotti, P., and Aebersold, R. (2012) Selected reaction monitoring-based proteomics: workflows, potential, pitfalls and future directions. *Nat. Methods* **9,** 555–566

47. Abbatiello, S. E., Schilling, B., Mani, D. R., Zimmerman, L. J., Hall, S. C., MacLean, B., Albertolle, M., Allen, S., Burgess, M., Cusack, M. P., Ghosh, M., Hedrick, V., Held, J. M., Inerowicz, H. D., Jackson, A., Keshishian, H., Kinsinger, C. R., Lyssand, J., Makowski, L., Mesri, M., Rodriguez, H., Rudnick, P., Sadowski, P., Sedransk, N., Shaddox, K., Skates, S. J., Kuhn, E., Smith, D., Whiteaker, J. R., Whitwell, C., Zhang, S., Borchers, C. H., Fisher, S. J., Gibson, B. W., Liebler, D. C., MacCoss, M. J., Neubert, T. A., Paulovich, A. G., Regnier, F. E., Tempst, P., and Carr, S. A. (2015) Large-scale inter-laboratory study to develop, analytically validate and apply highly multiplexed, quantitative peptide assays to measure cancer-relevant proteins in plasma. *Mol. Cell. Proteomics* M114.047050

48. Linder, A., Christensson, B., Herwald, H., Björck, L., and Åkesson, P. (2009) Heparin-binding protein: an early marker of circulatory failure in sepsis. *Clin. Infect. Dis.* **49,** 1044–1050

49. Stenemo, M., Teleman, J., Sjöström, M., Grubb, G., Malmström, E., Malmström, J. A., and Niméus, E. (2016) Cancer associated proteins in blood plasma: Determining normal variation. *Proteomics* **16,** 1928–1937

50. Schubert, O. T., Gillet, L. C., Collins, B. C., Navarro, P., Rosenberger, G., Wolski, W. E., Lam, H., Amodei, D., Mallick, P., MacLean, B., and Aebersold, R. (2015) Building high-quality assay libraries for targeted analysis of SWATH MS data. *Nat. Protoc.* **10,** 426–441

51. Escher, C., Reiter, L., MacLean, B., Ossola, R., Herzog, F., Chilton, J., MacCoss, M. J., and Rinner, O. (2012) Using iRT, a normalized retention time for more targeted measurement of peptides. *Proteomics* **12,** 1111–1121

52. Teleman, J., Röst, H. L., Rosenberger, G., Schmitt, U., Malmström, L., Malmström, J. A., and Levander, F. (2015) DIANA–algorithmic improvements for analysis of data-independent acquisition MS data. *Bioinformatics* **31,** 555–562

53. Ahrné, E., Molzahn, L., Glatter, T., and Schmidt, A. (2013) Critical assessment of proteome-wide label-free absolute abundance estimation strategies. *Proteomics* **13,** 2567–2578

54. Lange, V., Picotti, P., Domon, B., and Aebersold, R. (2008) Selected reaction monitoring for quantitative proteomics: a tutorial. *Mol. Syst. Biol.* **4,** 222

55. MacLean, B., Tomazela, D. M., Shulman, N., Chambers, M., Finney, G. L., Frewen, B., Kern, R., Tabb, D. L., Liebler, D. C., and MacCoss, M. J. (2010) Skyline: an open source document editor for creating and analyzing targeted proteomics experiments. *Bioinformatics* **26,** 966–968

56. Mi, H., Muruganujan, A., Casagrande, J. T., and Thomas, P. D. (2013) Large-scale gene function analysis with the PANTHER classification system. *Nat. Protoc.* **8,** 1551–1566